2010 International Conference on Industrial Electronics, Control and Robotics

Coupled Inductor Bidirectional DC-DC Converter for Improved Performance

Narasimharaju.B.L
Department of ElectricalEngineering
Indian Institute of Technology
Roorkee-247 667, India
E-mail: narasimharaju.bl@gmail.com

Satya Prakash Dubey
Department of ElectricalEngineering
Indian Institute of Technology
Roorkee-247 667, India
E-mail: spdubfee@iitr.ernet.in

S. P. Singh
Department of ElectricalEngineering
Indian Institute of Technology
Roorkee-247 667, India
Email: spseefee@iitr.ernet.in

Abstract—**Energy storage is the major concern in smart micro grids like in renewable power generation, electric vehicles and small scale DC-UPS systems. This paper proposes analysis, and voltage mode control of coupled inductor bidirectional converter. Unfortunately, switches of four and beyond in isolated schemes increase production costs and reduce conversion efficiency, and non-isolated topologies suffer from high voltage/current stress. As compared with the counterparts of conventional converter topologies, the proposed converter has the merits of less component count, high efficiency, and smaller size. The high voltage diversity enables a battery module of low voltage to be interfaced with the high-voltage dc bus or the micro grid for subsequent utilization. The battery fed bidirectional converter with controller to regulate the DC link voltage and battery charge voltage is implemented in the Simulink/Matlab environment. Also, experimental confirmation of the proposed converter is shown.**

Keywords- Bidirectional converter; Coupled inductor; Battery Storage System;

I. INTRODUCTION

An Electrical Energy Storage (EES) with anticipated unit cost reductions and hence their practical applications look very attractive for energy demands. Characteristics of small energy storage systems using storage batteries include the ability to install them in proximity to users, the promise of cost reduction through mass production, the ease of securing installation space, and the ability to combine UPS functions [8]. For this reason they are considered prime candidates for peaking power, standby reserve and load-balancing systems or peak-cut systems when used in conjunction with traditional sources of energy [6]. Generally it is more economical for storage batteries to use a few large-capacity cells than many small-capacity cells, and for that reason the number of cells used in small/micro power grid is limited. Usually, inverters used in DC-UPS (DUPS) systems require comparatively high input DC voltages of about 240V; which necessitates voltage step up when discharging batteries, and step down when charging them. Thus, batteries need high voltage diversity ratio in discharging, and charging modes. The authors propose a BDC circuit topology suited to which could be more attractive for micro/mini power grid in renewable energy conversion systems. The BDC employed in DUPS system incorporating battery bank has attracted special interest as promising load balancing system, and to meet failure situations of the mains power. This converter is capable of providing power flow in either direction while maintaining the polarities of the voltage on either side unchanged. Also, it proves to be scaled down energy storage system that replaces the bulk storage devices. These converters are widely used at vast varying power and voltage levels in many applications such as in DUPS system for battery charging/discharging, adjustable speed drives (ASDs), and AC grid interfacing system's etc. These BDCs are categorized as non-isolated BDCs [1]-[5] and isolated BDCs. The various isolated BDCs converters are reported in the literature, and also, BDCs with soft-switching techniques in order to reduce the switching loss and stress problems in [3]-[5]. However, those isolated and soft switching converters have the disadvantages such as more complicated, higher switch stress, instability due to high frequency transformer saturation, and less utilization of switch due to soft switching. The aforementioned complexities are not really encouraged to use in low or medium power applications. This paper mainly emphasizes on the improved changes of proposed BDC topology. This paper is includes four sections. Starting with Section I, the others sections cover the BDC operations and design analysis in Section-II, performance analysis in section-III, conclusive observations in Section-IV.

II. CONVERTER OPERATIONS AND DESIGN PRINCIPLES

The boost converter is a proven topology and is extensively used in industry as the unidirectional DC-DC converter stage for many high frequency inverter products, but not yet in bi-directional manner. Fig. 1 illustrates the conventional boost derived BDC circuit employed in DUPS system due to its simplicity, less components count, and simple controls [2, 3]. It is a transformer less type so as to reduce size and weight to improve economy [7]. The BDC topology operates in two modes. One is discharge mode during which the BDC is used to boost the battery voltage to a suitable high level DC bus voltage. Second is the charging mode during which the BDC is used to buck the DC bus voltage to a suitable low level battery voltage. The converter operation in continuous conduction mode (CCM) is a suitable choice to get a better dynamic response and also a tight regulation of output voltage for the entire load variation. In Fig. 1, during forward discharging mode Low Voltage (LV) side switch (S_1) operates and the converter acts as a boost converter; while during reverse charging mode, High Voltage (HV) side switch (S_2) operates and the converter acts as a buck converter [1, 2, 3].

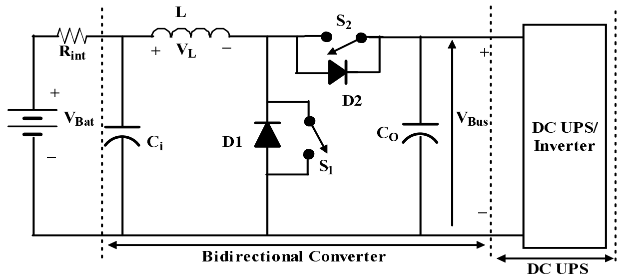

Figure 1. Bidirectional DC-DC converter feeding to DCUPS/inverter

For the conventional BDC shown in Fig. 1, the duty ratio (δ_1) of S_1 for step up, and the duty ratio (δ_2) of S_2 for step down operations are given by

$$\delta_1 = \frac{V_{Bus} - V_{Bat}}{V_{Bus}} \qquad \delta_2 = \frac{V_{Bat}}{V_{Bus}} \tag{1}$$

The currents of S_1 and D_2 during discharging mode are equal to battery discharge current, while the currents of S2 and D_1 during charging mode are equal to battery charging current, which means that S_1, S_2, D_l, and D_2 must be able to carry large currents. In both charging and discharging modes the applied voltages of S_1, S_2, D_l, and D_2 are equal to V_{Bus} (i.e. DC bus high-voltage) and hence all the devices must withstand high voltages. Thus, leads to low conversion efficiency.

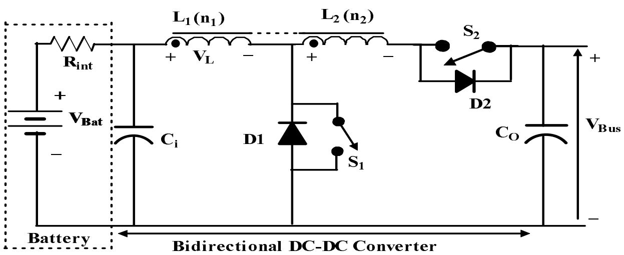

Figure 2. Proposed Bidirectional DC/DC converter

The configuration for the proposed bidirectional converter topology is depicted in Fig. 2. The characteristic waveforms of both boost and buck modes are depicted in Fig. 3. This proposed topology is quite similar to one reported in [1, 2, 3]. The major symbol representations are summarized as follows. V_{Bat} and V_{Bus}, respectively, denote the voltages at the low-voltage (LV) and high-voltage (HV), $L_1$and L_2 represent individual inductors in the primary and secondary sides of the coupled inductor respectively, where the primary side is connect to a battery module. The symbols S_1 and S_2 are the low-voltage step-up switch and high- voltage step-down switch respectively. When the power flows from the HV side to the LV side (switch S_2 is active), the circuit works in the buck state to recharge the battery from HV side or from absorbing regenerated energy. In the other direction of power flow, only triggering the low-voltage switch S_1, the circuit works in boost state to keep the bus voltage at a desired value. The proposed converter with coupled inductors appreciably reduction in the voltage and current stress of the power switches. Thus, this paper discusses the operating and design principles, and other aspects of the proposed converter shown in Fig. 2. In this study, the following assumptions are made to simplify the converter analyses: 1) All MOSFETs (including their body diodes) are assumed to be ideal switching elements. 2) The conductive voltage drops of the switch and diode are neglected. 3) Delay time (t_d) is assumed to be negligible 4) Negligible battery internal resistance voltage drop. Using this proposed bidirectional DC-DC converter topology one can retain all the benefits of conventional boost topology in addition to the high conversion efficiency and reduced switching stress. The converter design and analyses procedure in the buck and boost states are described in the following subsections.

A. Forward Boost Mode

When the proposed converter operates in the boost state, the power flow is from the battery to the HV DC bus. The characteristic waveforms in the boost state are depicted in Fig. 3 and the topological modes in one switching cycle are illustrated in Fig. 4.

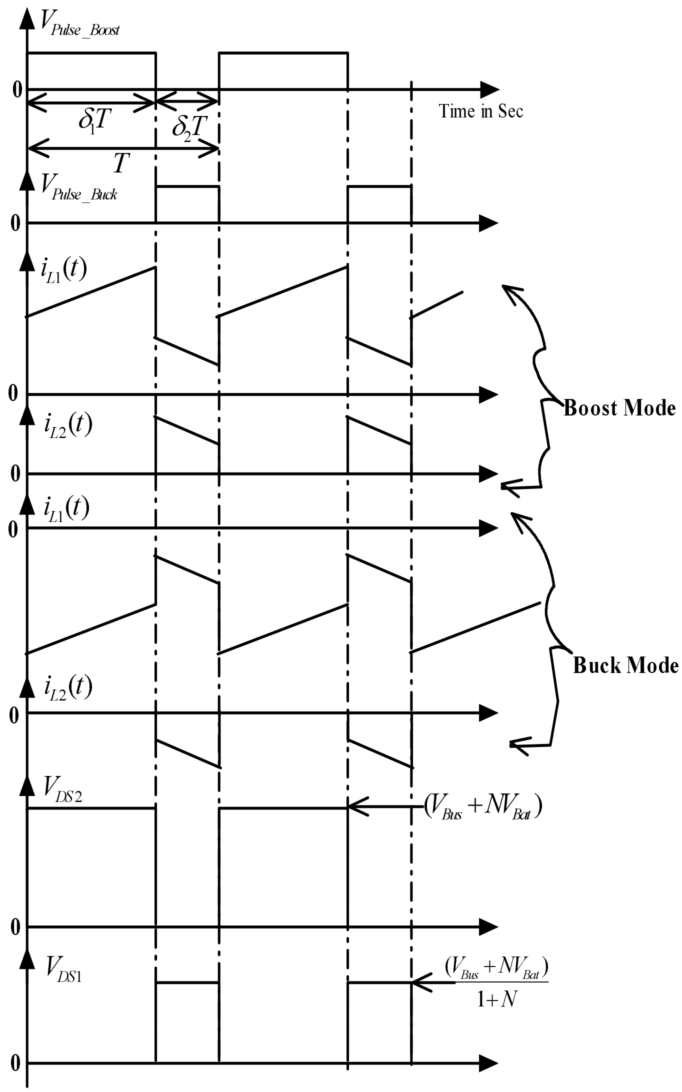

Figure 3. Ideal waveforms of proposed BDC in boost mode and buck mode

Mode-1[Fig. 4(a)]: In this mode, the LV side switch (S_1) is conducting for T_{ON} time. Because the inductor is charged by the battery, the magnetizing current increases gradually in an approximately linear way. The primary voltage is given by

$$V_{L1} = V_{Bat} = L_1 \frac{di_{L1}}{dt} = L_1 \frac{\Delta i_{L1}}{\Delta t_{S1ON}} \qquad (2)$$

The secondary current is zero since diode D_2 is reverse biased. The secondary inductor induced voltage is $V_{L2} = NV_{L1}$ and the turns ratio $N = \frac{n_2}{n1}$. Where, n_1 and n_2 are the primary (L_1) and secondary (L_2) winding turns of the coupled inductor.

Mode-2[Fig. 4(b)]: In this mode, the LV side switch (S_1) is turned off for T_{OFF} time. Thus reverses the polarities of the coupled inductors. The diode D_2 gets forward biased and the mode begins when the primary current equals the secondary current. The battery and the coupled inductor are connecting in series to discharge into the HV DC bus through the Diode D_2 by way of a low current type. Since, the inductor is supplied to the DC bus, the magnetizing current decreases gradually in an approximately linear way. The primary voltage is given by

$$V_{L1} = \frac{(V_{Bus} - V_{Bat})n_1}{n_1 + n_2} = (L_1 + M)\frac{\Delta i_{L_1}}{\Delta t_{S1OFF}} \qquad (3)$$

Where, $\Delta t_{S1OFF} = (1-\delta_1)T$, T is the switching period and δ_1 is the duty cycle of switch S1.

Average voltage across the inductor L_1 is zero over a switching period ($T = T_{ON} + T_{OFF}$); by simplifying the Eq.(2) and Eq.(3), the DC gain of the boost mode is developed as follows;

$$G_1 = \frac{V_{Bus}}{V_{Bat}} = \frac{(1 + N\delta_1)}{(1 - \delta_1)} \qquad (4)$$

The duty cycle δ_1 can be calculated from Eq.(4).

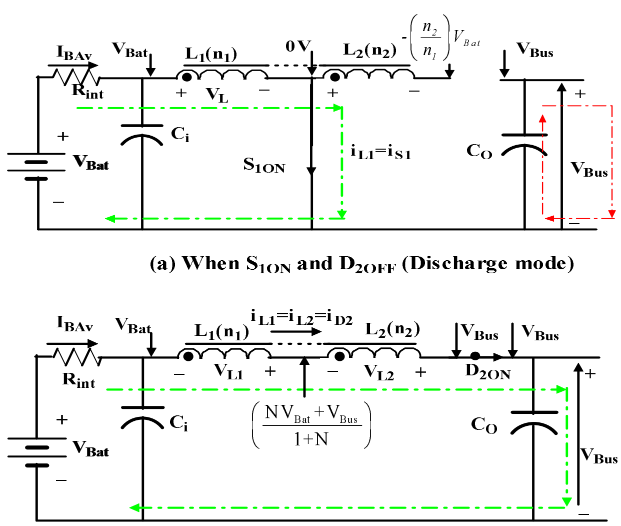

(a) When S_{1ON} and D_{2OFF} (Discharge mode)

(b) When S_{1OFF} and D_{2ON} (Discharge mode)

Figure 4. Equivalent circuits of proposed BDC for boost and buck mode

B. Reverse Buck Mode

The characteristic waveforms of the proposed converter in the buck state are depicted in Fig. 3 and the topological modes in one switching cycle are illustrated in Fig. 4. The coupled inductor in Fig. 2 can be modeled as an ideal transformer including the magnetizing inductors (L_{m1} and L_{m2}) and leakage inductors (L_{k1} and L_{k2}) those are not shown in the figure. The coupling coefficients (k_1 and k_2) of ideal transformer are defined as

$$k_1 = \frac{L_{m1}}{(L_{m1} + L_{k1})} = \frac{L_{m1}}{L_1} \quad k_2 = \frac{L_{m2}}{(L_{m2} + L_{k2})} = \frac{L_{m2}}{L_2} \qquad (5)$$

The coupling coefficients is simply set at one to obtain $L_{m1}=L_1$ and $L_{m2}=L_2$ via Eq.(5).

Mode 1 [Fig. 4(b)]: In this mode, the HV side switch (S_2) is turned on and the other switch is turned off for a span. Both the diodes are reverse biased. The secondary current (I_{L2}) is from the HV bus by way of the two series windings ($L_1$and L_2) of the coupled inductor to charge the battery in the LV side. At this time, the series windings ($L_1$and L_2) and their mutual inductance (M) can be taken as a single inductor, and the equivalent magnetizing inductor (L_m) can be represented as

$$L_m = (1+N)^2 L_1 = (1+\frac{1}{N})^2 L_2 = (L_1 + L_2 + 2M) \qquad (6)$$

Mutual inductance $M = K\sqrt{L_1 L_2} = NL_1$ for 100% coupling (i.e. K=1) the equivalent inductor (L) is larger than the value of (L_1 or L_2) to limit the ripple and ascendant rates of the charge current, and its voltage can be described as

$$L_m \frac{di_L}{dt} = (V_{Bus} - V_{Bat}) \qquad (7)$$

Applying Kirchhoff's voltage law, the voltage V_{Bus} is given by

$$V_{Bus} = V_{L2} + V_{L1} + V_{Bat} = V_{L1}(1 + N) + V_{Bat} \qquad (8)$$

Where, V_{L1} and V_{L2} are the voltages across the primary and secondary windings of the coupled inductor.

When S_2 is conducting, the inductor voltage (V_{L1}) is described as follows

$$V_{L1} = \frac{(V_{Bus} - V_{Bat})n_1}{n_1 + n_2} = (L_1 + M)\frac{\Delta i_{L_1}}{\Delta t_{S2ON}} \qquad (9)$$

Where, $\Delta t_{S2ON}=(1-\delta_1)T= \delta_2 T$ and δ_2 is the duty cycle of switch S_2.

Mode 2 [Fig. 4(a)]: In this mode, the HV side switch (S_2) is turned off and the diode D_1 is forward biased. The polarities of the coupled inductors are now reverse. The primary current (I_{L1}) is flows through the diode D_1, primary inductor (L_1) to charge the battery in the LV side. The voltage across the primary winding L_1 is given by

$$V_{L1} = V_{Bat} = L_1 \frac{\Delta i_{L_1}}{\Delta t_{S2OFF}} \quad (10)$$

Average voltage across the inductor L_1 is zero over a period ($T=T_{ON}+T_{OFF}$); by simplifying the Eq.(9) and Eq.(10), the DC gain of the buck mode developed as follows:

$$G_2 = \frac{V_{Bat}}{V_{us}} = \frac{\delta_2}{(1+N(1-\delta_2))} \quad (11)$$

The duty cycle δ_2 of switch S_2 can be calculated from (11), the relationship between δ_1 and δ_2 must satisfy the condition $\delta_1 + \delta_2 = 1$. The device currents are obtained based on the power balance relation with negligible losses as follows;

$$V_{Bat} I_{BAv} = V_{Bus} I_{BuAv} \quad (12)$$

$$I_{BAv} = \delta_1 I_1 + I_2(1-\delta_1) \quad (13)$$

$$I_1 + = I_2(1+N) \quad (14)$$

Where, I_{BAv} and I_{BuAv} are the average battery current and the DC-Bus (HV) current respectively.

By simplifying the equations (12) to (14) Peak current through S_1/D_1 and S_2/D_2 are obtained as follows;

$$I_1 = I_{BAv} + NI_{BuAv} \quad (15)$$

$$I_2 = \frac{I_{BAv} + NI_{BuAv}}{(1+N)} \quad (16)$$

According to the voltage-second balance, from Fig. 4(b) and Fig. 5(a), voltage applied to the switch $S_1$and the diode D_1 in their OFF states is obtained as

$$V_{DS1} = V_{L1} + V_{Bat} = \frac{(V_{Bus} + NV_{Bat})}{(N+1)} \quad (17)$$

Similarly, from Fig. 4(a) and Fig. 5(b), voltage applied to the diode D_2 or the switch S_2 in their OFF states is obtained as

$$V_{DS2} = V_{L2} + V_{Bus} = (V_{Bus} + NV_{Bat}) \quad (18)$$

Table-I describes the comparative study of conventional and the proposed BDCs in terms of the switch voltages, currents and duty ratios calculated theoretically.

TABLE-I. CONVERTERS PARAMETER COMPARISONS

BOOST MODE	BUCK MODE	CONVENTIONAL	PROPOSED
S_1 VOLTAGE	D_1 VOLTAGE	200V	82.67V
S_1 CURRENT	D_1 CURRENT	16.67A	20.67A
S_2 VOLTAGE	D_2 VOLTAGE	200V	248V
S_2 CURRENT	D_2 CURRENT	16.67A	6.89A
S_1 DUTY	-----	88%	71%
-----	S_2 DUTY	12%	29%

C. Design Considerations and Analysis

In continuous current conduction the minimum current carried by the inductor L_1 is represented as

$$i_{L1\min} = I_{BAv} - \frac{\Delta i_{L1}}{2} \quad (19)$$

Using, Eq.(3) in Eq.(19) under boundary current conduction mode (i.e. $i_{L1\min} = 0$); the minimum value of inductance (L_1) can be obtained as

$$L_{1\min} = \frac{V_{Bat} R_{Bus} (V_{Bus} - V_{Bat})(1-\delta_1)T}{2V_{Bus}^2 (N+1)} \quad (20)$$

For continuous current conduction the selected value of $L_1 >>> L_{1\min}$ and vice versa for discontinuous current conduction. Finally equivalent inductance (L_m) and secondary coupled inductor (L_2) can be calculated from Eq.(6). In Fig. 2 the filter capacitors C_i and Co are used on the LV battery side and HV DC-bus side respectively to achieve constant voltages. These capacitors can be calculated based on the desired ripple voltages. Substituting N= 1 ~ 4 into Eq.(4), the curve of the voltage gain (G_1) with respect to the duty cycle (δ_1) is depicted in Fig. 5. As can be seen from this figure, the voltage gain of the proposed converter with a boost type is higher than conventional single-inductor-based converter [2], especially for lower value duty cycle. Also, substituting N= 1 ~ 4 into (11), the curve of the voltage gain (G_2) with respect to the duty cycle (δ_2) is depicted in Fig. 6. As can be seen from this figure, the voltage gain of the proposed converter is regulated via the conduction rate of the high-voltage switch (S_1), and the stable region of the duty cycle (δ_2) is from zero to its maximum point. Hence, according to the manipulation of $\frac{\partial G_2}{\partial \delta_2} = 0$ the maximum controllable duty cycle δ_{2max} can be obtained. By analyzing Figs. 5 and 6, the turns ratio of the coupled inductor is selected as N=2 when the operational conditions are V_{Bat}=24V and V_{Bus}=200V. Consequently, the corresponding duty cycles can be obtained as δ_1=0.71 and δ_2=0.29 from Eq.(4) and Eq.(11). These values are reasonable in practical applications.

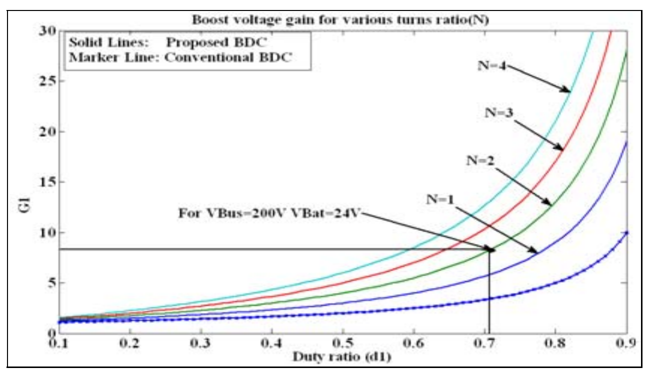

Figure 5. Voltage gain (G_1) with respect to duty cycle (δ_1) under different turn's ratios

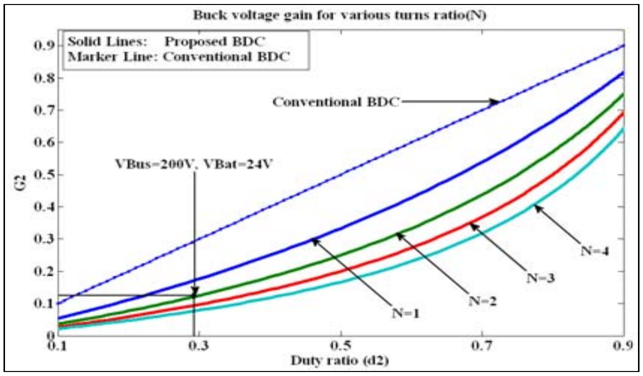

Figure 6. Voltage gain (G_2) with respect to duty cycle (δ_2) under different turn's ratios

III. PERFORMANCE ANALYSIS

The conventional and proposed BDC schematics for simulation with following specifications are designed to illustrate the design procedure given in Section-II: LV side V_{Bat}=24±2V, HV side V_{Bus}=200±18V, HV side power is 400W and LV side power is 250W. Fig. 7(a) and Fig. 7(b) illustrate the Simulink models of the conventional and proposed BDC converters respectively. In these schematics a low-pass filter capacitors C_i and C_o of 100 μF are used to in order to maintain the constant charging voltage and constant bus voltage. For the realistic simulation of battery charging/discharging application, the other designed parameter values are as follows: L=50μH for the conventional BDC and for proposed BDC L_1=29μH L_2=116μH with coupling coefficient (K) of 0.98. Fig. 8 and Fig. 9 illustrate the steady-state simulation results of the conventional BDC for varying loads. Fig. 10 and Fig. 11 illustrate the steady state response of proposed BDC. Simulated result has a close agreement with the theoretically designed parameter values. Fig. 12 illustrates the experimental validations of the proposed coupled inductor BDC converter that confirming the improvements of the proposed topology providing with minimum current and voltage stresses.

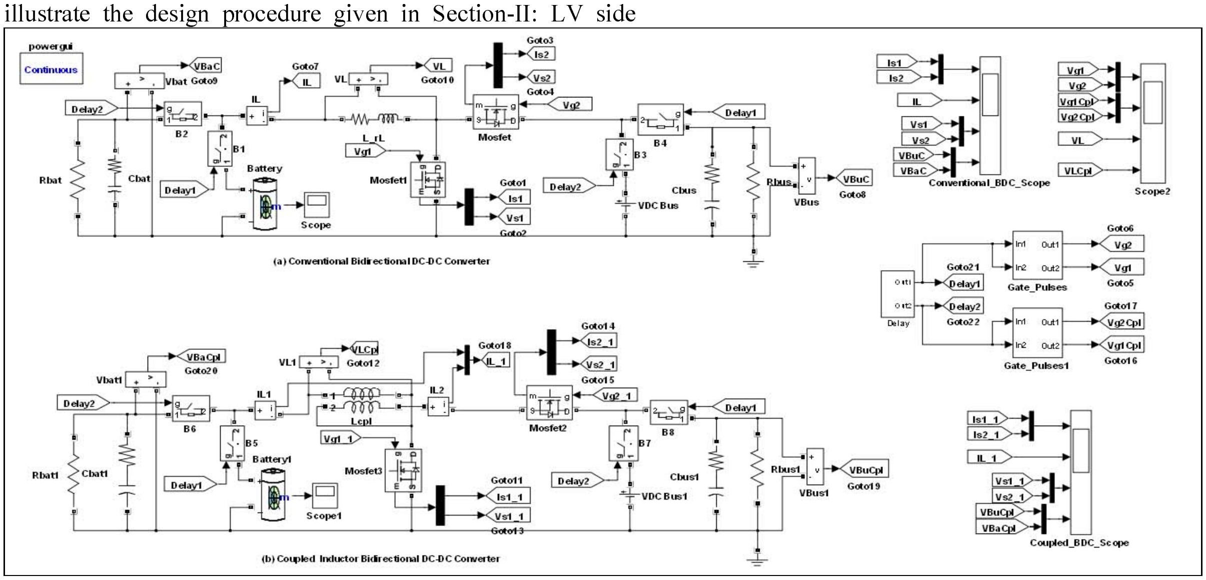

Figure 7. Simulink schematics (a) Conventional BDC, (b) Coupled BDC

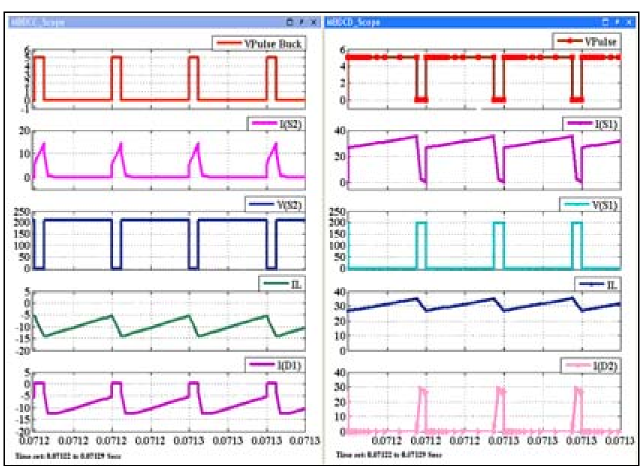

Figure 8. Waveforms of conventional BDC: V_{Pulse}, I_{Switch}, V_{Switch} and I_L in Buck Mode (signals with Marker) and Boost Mode (Signals without Marker)

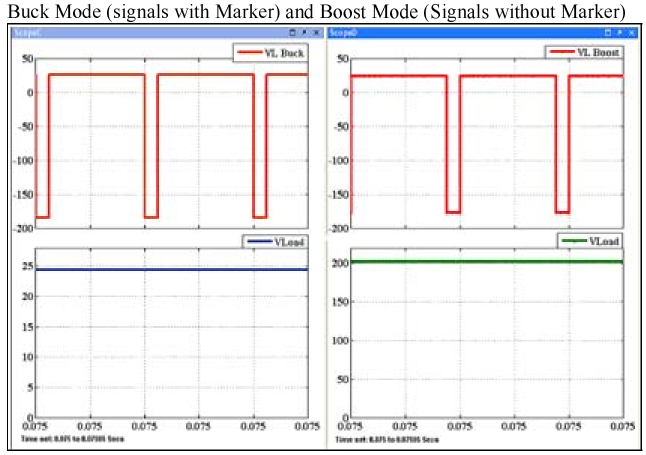

Figure 9. Waveforms of conventional BDC: Inductor (L_1) voltages and Load voltages in Buck Mode (signals with Marker) and Boost Mode (Signals without Marker)

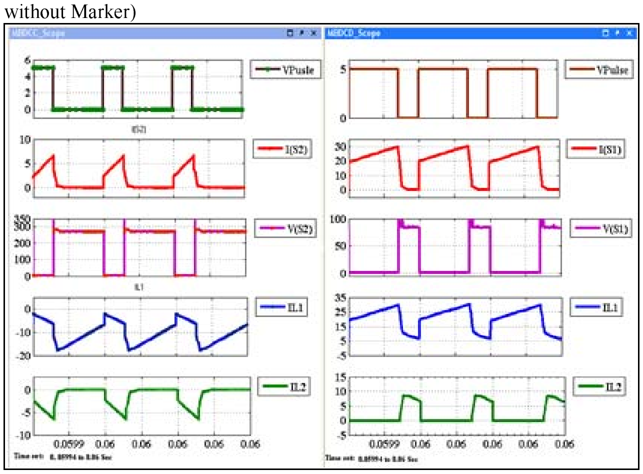

Figure 10. Waveforms of coupled BDC: V_{Pulse}, I_{Switch}, V_{Switch} and I_L in Buck Mode (signals with Marker) and Boost Mode (Signals without Marker)

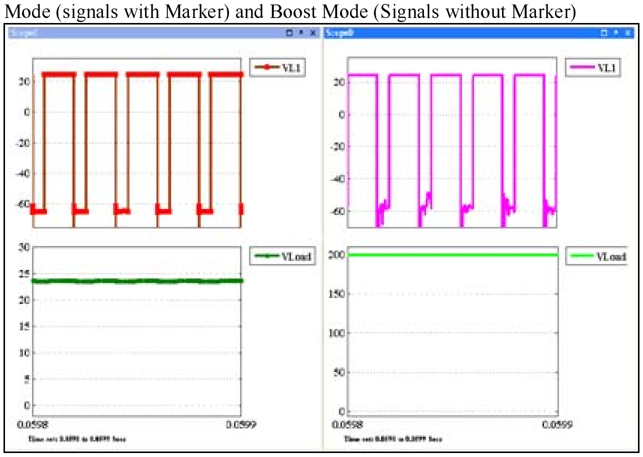

Figure 11. Waveforms of proposed BDC: Inductor (L_1) voltages and Load voltages in Buck Mode (signals with Marker) and Boost Mode (Signals without Marker)

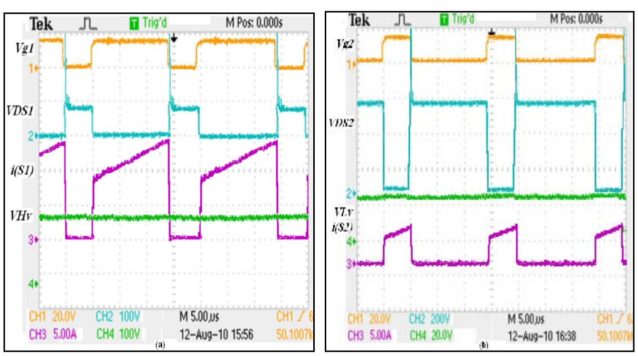

Figure 12. Steady state experimental performances of proposed BDC converter (a) boost mode at full load; Ch1:20v/div, Ch2:100v/div, C3:10A/div and Ch4:100V/div, (b) buck mode at full load; Ch1:20v/div, Ch2:100v/div, C3:10A/div and Ch4:20V/div

IV. CONCLUSION

The theoretical design analysis has been made, and also design considerations are discussed. The steady-state analysis of conventional and proposed BDCs has been made in Simulink environment. Also, experimental validation of the proposed BDC is given. The results and analysis reveals that the one third reduction in LV side switch (S1) voltage stress, HV side switch (S2) current stress, and also switch utilization factor of the proposed BDC than that of conventional BDC. Thus, the proposed BDC assures superior than that of the conventional BDC. The newly designed converter circuit offers the following improvement over those reported elsewhere. 1) This topology adopts only two switches to achieve the objective of bidirectional power flow. 2) The voltage gain and the utility rate of the magnetic core can be substantially increased by using a coupled inductor with a lower turn's ratio. Hence, the coupled inductor BDC converter provides high voltage diversity than that of the conventional BDC converter. Therefore, the proposed coupled inductor BDC is the good choice where isolation is not the critical issue like in DC-UPS systems.

REFERENCES

A. Jusoh, A. J. Forsyth and Z. Salam, "Analysis and Control of the Unloaded Bi-directional DC/DC Converter to Perform an Active Damping Function," Jurnal Teknologi, 44(D) (JTjun44D[5]CRC.pmd), pp. 65-84, June 2006.

Chang Gyu Y, Woo-Cheol L, Kyu-Chan L and Bo H Cho, "Transient Current Suppression Scheme for Bidirectional DC-DC Converter in 42V Automotive Power systems, Conf. Rec. of IEEE 2005, pp.1600-1604.

D. Diaz, and O. Garcia, et al., "Analyzes and Design considerations for the right half-plane zero cancellation on a boost derived dc/dc converter," IEEE Transactions, pp. 3825-3828, 2008.

S. Waffler and I.W. Kolar, "A Novel Low-Loss Modulation Strategy for High-Power Bi-directional Buck Boost Converters", 7Th International Conf. on Power Electronics-07, PP.889-894, Oct 2007.

Y. S. Lee, and G. T. Cheng, "Quasi-Resonant Zero-Current-Switching Bidirectional Converter for Battery Equalization Applications," IEEE TRANS on Power Electronics, vol.21, no.5, Sept-2006, PP-1213-1224

R. J. Wai and R. Y. Duan, "High-efficiency dc/dc converter with high voltage gain," Proc. Inst. Elect. Eng., vol. 152, pp. 793–802, 2005.

Baker. J. N and Collinson, "A Electrical energy storage at the turn of the millennium", Power Eng 1999, pp.107-12.

Yoshihiko Yamakata, and Makoto Yatsu, et al., "Development of New Series MINI-UPS', Tran. of Japan Society for Power Electronics, V01.25, No.1, pp.81-89, 1999.

Kaiwei Yao, Mao Ye, Ming Xu and Lee F.C, "Tapped-inductor buck converter for high-step-down DC-DC conversion", IEEE Transactions on Power Electronics, Vol. 20, Issue 4, pp. 775-780, 2005.

M. Rico, J. Uceda, J. Sebastian, and F. Aldana, "Static and dynamics modeling of tapped-inductor DC-to-DC converters," in *Proc. IEEE PESC'87*, 1987, pp. 281–288.